# Integrated all-fiber variable optical attenuator based on index-guiding holey fiber

**Youngbok Kim,[a] Kyunghwan Oh,[b] and Chang-Soo Park[a]**
[a]Gwangju Institute of Science and Technology (GIST), Department of Information and Communications, 1 Oryong-dong, Buk-gu, Gwangju, 500-712, South Korea
E-mail: csp@gist.ac.kr
[b]Yonsei University, Institute of Physics and Applied Physics, Seoul 120-749, South Korea

**Abstract.** We report an integrated all-fiber variable optical attenuator (VOA) for dynamic control of a device by achieving optimized taper and axial compression of an index-guiding holey fiber. We experimentally demonstrate a VOA device with dynamic ranges of 18 dB over the spectral range from 1450 to 1650 nm and a low insertion loss of 0.5 dB. © *2008 Society of Photo-Optical Instrumentation Engineers.*
[DOI: 10.1117/1.2829585]

## 1 Introduction

Index-guiding holey fiber (IGHF) has had intense attention due to its novel waveguide properties, which are different from those conventional single-mode fiber in terms of high nonlinearity,[1] large chromatic dispersion,[2] and wide single-mode operation.[3] IGHF contains the periodic arrangement of air holes that run continuously along the length of the fiber, and recently it is investigated in all-optical sensor applications.[4] Numerous types of tunable optical devices are being proposed for optical communication systems including optical tunable filters,[5] switches,[6] and all-fiber variable optical attenuators[7,8] (VOAs). The tunability of a device for potential sensor applications must be accomplished by meeting essential requirements such as low insertion loss, high dynamic range, and low polarization-dependent loss (PDL). These characteristics can be easily obtained in all optical fiber devices, bulk optics, and planer waveguides devices.

In this letter, we demonstrate an integrated all-fiber tunable optical device with a simple process based on an adiabatically tapered IGHF. We report coupling and loss characteristics of the tapered IGHF and demonstrate a VOA as a tunable device with about a 18-dB dynamic range over a spectral range of 200 nm and with a low insertion loss of 0.5 dB.

## 2 Design and Properties

To achieve efficient field interaction between the core and air holes, the IGHF is adiabatically tapered by heating and elongating the fiber such that the outer diameter decreases while the cross-sectional profile remains approximately the same. Thus, we apply a flame brushing technique that was applied to provide a hot zone where fibers are fused and elongated by electrically motorized stages.

For an adiabatic and low-loss design, the IGHF takes into account the mode properties at different dimensions. In the IGHF, the light is initially coupled into the fundamental core mode, and the main loss mechanism is through coupling of energy to the fundamental space-filling mode (FSM) of the microstructure. We can calculate the propagation constants of the core and space-filling modes $\beta_{core}$ and $\beta_{FSM}$ using the plane wave expansion method and applying them to the adiabatic criterion for the low-loss mechanism. Then it is applied to an IGHF with an infinite microstructure:

$$\left| \frac{dr}{dz} \right| \le \frac{r(\beta_{core} - \beta_{FSM})}{2\pi},$$

where $r(z)$ is the longitudinal variation in the fiber dimensions. For the preceding criterion to apply, the cross-sectional image of IGHF is preserved when tapered.

Figure 1(a) shows a cross-sectional image of the IGHF, which has an outer diameter of 125 $\mu$m and a core surrounded by four layers of air holes with a pitch period of 6.4 $\mu$m, having different air-hole diameters of 3.8, 4.4, 5, and 5 $\mu$m. Figure 1(b) shows the adiabatic transformation of IGHF, which is scaled down proportionally along the fused region. In the tapered region of the IGHF, the diffraction causes fundamental mode escape from the core so that the input power is coupled and trapped into the cladding mode. As a result, the output power from the tapered IGHF is attenuated.

## 3 Experiment and Results

Figure 2(a) shows a cross-sectional image of the adiabatically tapered IGHF whose outer diameter is 115 $\mu$m. To measure the attenuation characteristics with axial compression on the tapered and fixed IGHF, we set up the measurement system shown in Fig. 2(b). For this experiment, we used a computer-controlled and high-precision motorized stage with nanometer resolution as a microactuating platform (MAP) to provide the axial compression. The microoptical waveguide (MOW) was then assembled on the MAP by steadfast fiber holders to form a MOW on MAP structure, where the axial compression can be accurately applied over the tapered region.

Figure 3(a) shows the loss profile of the adiabatically tapered IGHF before compression, which has an elongation length of 0.5 mm. The spectrum range measured was from about 1450 to 1650 nm, and the loss profile dropped down more in the shorter wavelength than in the longer wavelength in the IGHF. To measure the axial compression characteristic of the IGHF, we gradually compressed the tapered IGHF with in 2-$\mu$m intervals, and the totally compressed length was increased up to 20 $\mu$m using the motorized stage. Figure 3(b) shows the attenuation curves measured with at 2-$\mu$m intervals, showing a linear increase from −0.5 to −18 dB over the spectral range from 1450 to 1650 nm. The top profile in Fig. 3(b) is the same curve as that of Fig. 3(a), i.e., before axial compression. To investigate
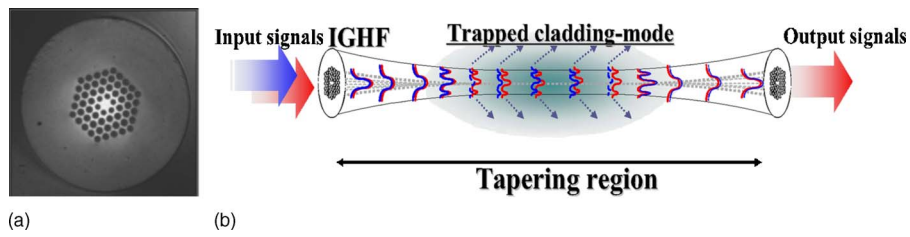
**Fig. 1** (a) Schematic diagram of the cross-sectional image of IGHF and (b) schematic diagram of the adiabatically tapered IGHF.
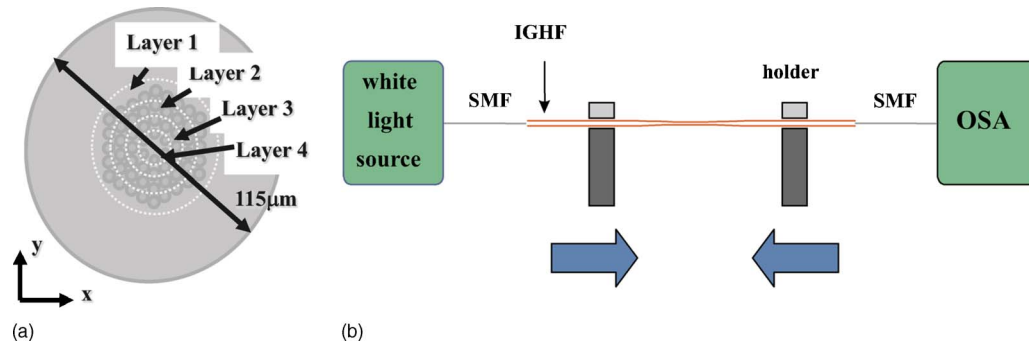


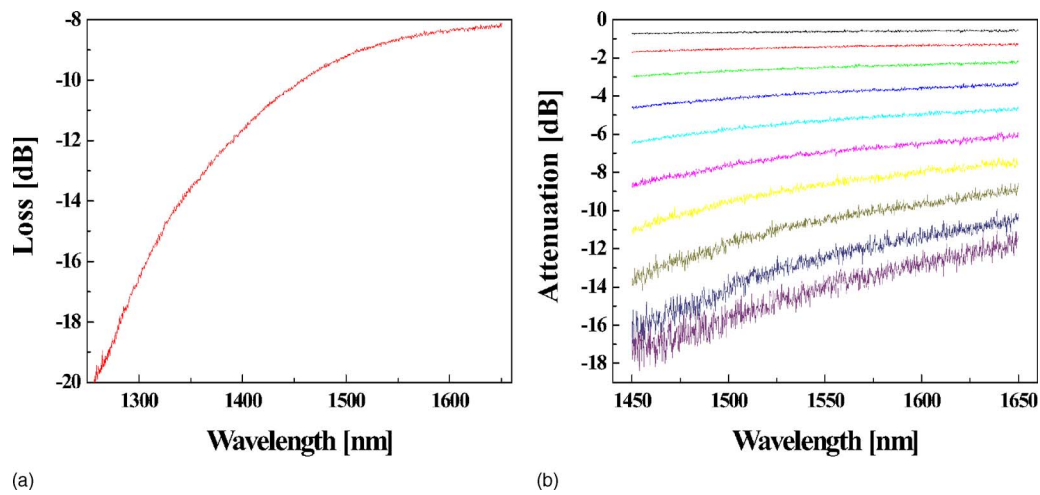**Fig. 2** (a) Cross-sectional image of the tapered IGHF and (b) setup for the axial compression.



**Fig. 3** (a) Loss profile of the tapered IGHF and (b) attenuation profiles of the compressed IGHF with increases in 2-$\mu$m steps.
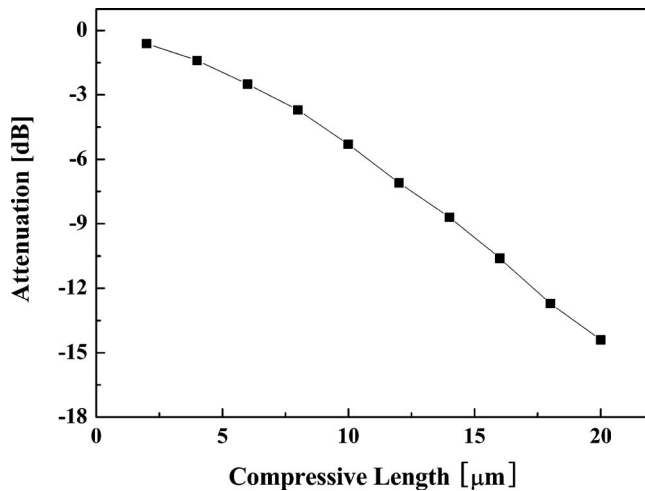
**Fig. 4** Attenuation curve of the compressed IGHF with an increase in compressive length at 1550 nm.

wavelength-dependent attenuation, other attenuation curves were normalized to the top curve as reference spectra and were plotted.

Figure 4 shows the attenuation characteristics as a function of compressed length at a wavelength of 1550 nm. The output power was gradually attenuated with an increase in compressive length, showing an accuracy of about 0.9 dB with a compression of 1 $\mu$m. The repeatability of the IGHF measured at the same wavelength appeared to be within $\pm 0.6$ dB for the lowest attenuation curve of Fig. 3(b). We measured the temperature-induced variation in attenuation to room temperature, maintaining the tapered IGHF at 85°C on a thermal electric cooler. The output power was reduced by 0.16 dB over 60°C, resulting in slightly more attenuation.

Note that the output power was linearly decreased below $-18$ dB over the wide wavelength range from 1450 to 1650 nm. The fabricated VOA showed a low insertion loss of 0.5 dB and a simple fabrication process with integrated all-fiber based on tapered IGHF.

## 4 Conclusion

An integrated all-fiber VOA spectrum response was achieved in the adiabatic tapers of IGHF. The optimized spectrum was achieved by the adiabatically flame brushing technique with an elongation length of 0.5 mm. With the axial compression, a novel attenuation characteristic was obtained over the spectral range from 1450 to 1650 nm, showing linear increase from $-0.5$ to $-18$ dB.

### References

1. J. K. Ranka, R. S. Windeler, and A. J. Stentz, "Visible continuum generation in air silica microstructure optical fibers with anomalous dispersion at 800 nm," *Opt. Lett.* **25**, 25–27 (2000).
2. J. Broeng, D. Mogilevstev, S. E. Barkou, and A. Bjarklev, "Photonic crystal fibers: a new class of optical waveguides," *Opt. Fiber Technol.* **5**, 305–330 (1999).
3. T. A. Birks, J. C. Knight, and P. St. J. Russel, "Endlessly single-mode photonic crystal fiber," *Opt. Lett.* **22**, 961–963 (1997).
4. J. B. Jensen, J. Riishede, J. Broengx, J. Laegsgaard, T. Tanggaard Larsen, T. Sorensen, K. Hougaard, E. Knudsen, S. B. Libori, and A. Bjarklev, "Photonic crystal fibers; fundamental properties and applications within sensors," in *Sensors, 2003, Proc. IEEE*, Vol. **1**, pp. 269–278 (2003).
5. I. D. Villar, I. R. Matías, and F. J. Arregui, "Fiber-optic multiple-wavelength filter based on one-dimensional photonic bandgap structures with defects," *J. Lightwave Technol.* **22**, 1615–1621 (2004).
6. P. Petropoulos, T. M. Monro, W. Berlardi, K. Furusawa, J. H. Lee, and D. J. Richardson, "2 R-regenerative all-optical switch based on a highly nonlinear holy fiber," *Opt. Lett.* **26**, 1233–1235 (2001).
7. C. Kerbage, A. Hale, A. Yablon, R. S. Windeler, and B. J. Eggleton, "Integrated all-fiber variable attenuator based on hybrid microstructure fiber," *Appl. Phys. Lett.* **79**, 3191–3193 (2004).
8. H. Zhang, Y. Liu, L. Yu, G. Zhou, S. Yuan, and X. Dong, "Novel all-fiber variable optical attenuator based on high-birefringence fiber loop mirror," *Proc. SPIE* **5279**, 456–460 (2004).